2014 IEEE International Conference on Robotics & Automation (ICRA)
Hong Kong Convention and Exhibition Center
May 31 - June 7, 2014. Hong Kong, China

Model-Free Force Tracking Control of Piezoelectric Actuators: Application to Variable Damping Actuator

Jinoh Lee, Matteo Laffranchi, Navvab Kashiri, Nikolaos G. Tsagarakis and Darwin G. Caldwell

Abstract— **On a new demand of safe human-robot interaction for robotic applications, the Compact Compliant Actuator, named CompAct™, is recently developed with physical compliance and active variable damping. In this mechanism, a desired physical damping behavior is realized by generating a friction force which is actively controlled by piezoelectric actuators (PEAs). However, nonlinearities such as hysteresis and creep effect make difficult to precisely control the generated piezoelectric force. This paper focuses on a development of precise force tracking controller for PEAs. A time delay estimation (TDE) using a force feedback is newly proposed to compensate a hysteretic behavior of the PEA and external uncertainties without a mathematical model. Thanks to the force-based TDE, the proposed control is accurate, computationally efficient and easily implementable on the real PEA system. The proposed control scheme is experimentally verified on the CompAct™. Root-mean-square values of the steady-state error for step commands are kept as less than error ratio of 0.13 % and the closed-loop system bandwidth for sinusoidal commands of 20 N stroke is confirmed as about 11 Hz under 100 N payload. In addition, the stability of the proposed control is proved to be bounded-input-bounded-output (BIBO) stable.**

I. INTRODUCTION

An emerging technology in the use of industrial-coworkers and service robots is to introduce a physical compliance inside the robot's structure [1], [2]. Classical stiff and heavy manipulators with high-gain controllers are not suitable to operate close to a human and physically interact with the surrounding environment. This is because conventional design and control approach make robots difficult to interact with its surroundings due to the large output mechanical impedance which results in lack of robustness [3] and safety [4]. Furthermore, other aspects can be jeopardized by this actuation approach, e.g., energy efficiency [5].

This safety concern during human-robot interaction has lead to the recent development of the Compact Compliant Actuator, CompAct™, where semi-active dampers/clutches are incorporated into the compliant actuator design [6]–[8]. While the compliance is necessary to enable robots to work in unstructured environments, it introduces several non-ideal effects, e.g., under-damped dynamics limit the achievable bandwidth of the controlled system; or oscillations radically deteriorate an accuracy of the robot and might lead to unstable behaviour [9], [10]. The semi-active damper in CompAct™ assists in overcoming the limitations introduced by the physical compliance in the actuator. Given that integration density is paramount in most robotic designs, the ideal actuator to drive the semi-active dampers must show high force density, lightweight and an overall compact size. A piezoelectric actuator (PEA) is certainly compatible with such characteristics [11] and it has been used previously to control the force generated by the semi-active damper in [7]. In that work the force-regulated piezoelectric actuators constitute an inner loop of a nested loop control architecture and is therefore the basis of the whole control scheme significantly affecting its performance. Accordingly, an accurate force control performance is particularly important in this application of variable physical damping actuator.

The forces created by PEA are generated by controlling the drive voltage and exploiting the "piezoelectric effect." However, PEA exhibits strong nonlinearities such as a hysteresis, since materials of the PEA are generally ferroelectric. To obtain high control accuracy for the PEAs and to remove unwanted harmonics in the closed-loop system, the hysteresis effect must be compensated. There have been several approaches to linearize PEAs using model-based compensation strategies [12]–[15]. More specifically for force control, the PEA models have been incorporated into discrete proportional-integral (PI) control [16], sliding-mode control (SMC) [17] and H-∞ control [18]. However, it is difficult or time-consuming to obtain an exact mathematical model and to identify system parameters of the model due to the highly nonlinear and complicated dynamics of the hysteresis effect. To mitigate this difficulty, other methods investigated include use of neural networks [19], [20] and disturbance observers (DOB) with SMC [21]: for the former, the external force on the PEA is supposed to be zero or constant, which is a satisfactory assumption for the position tracking control; and for the latter, the controller needs an additional force observer with DOB and the SMC uses the second derivative of the force, which is normally undesirable. Thus, there is still a need to develop force control which is easy to implement, efficient in real-time control basis, and robust against nonlinearities.

As a such technique, we propose a precise model-free force tracking controller based on a force-based time delay estimation (TDE) and a simple proportional-derivative (PD) force feedback control. The TDE was originally developed to compensate nonlinear terms and uncertainties of robot manipulator dynamics [22] and its efficiency and effectiveness has been theoretically and practically proven in previous researches [23], [24]. While the original TDE uses intentionally time-delayed information of a control torque and an acceleration at the previous time step, we propose the force-based TDE which uses force feedback and control

The authors are with Department of Advanced Robotics, Istituto Italiano di Tecnologia (IIT), Via Morego 30, 16163, Genova, Italy jinoh.lee@iit.it

voltage values at the previous time step to cancel nonlinear hysteresis and other uncertainties of PEAs. Endowed by the characteristic of the TDE, the proposed force control provides accurate and robust tracking performance, while it needs neither expensive computation nor off-line identification process. In addition, the PD-type servo control makes a transient force response fast but smooth with a minimal information using only a force measurement.

Therefore, the contribution of this paper is to develop a precise, yet efficient and robust force tracking control for PEAs which can satisfy the requirements of practical applications. We propose the force-based TDE to compensate the nonlinearities of PEA such as the hysteresis effect, without mathematical models and strive to show its stability in a rigorous manner. The proposed controller is physically implemented on the CompAct^{TM} system. Through experiments, its tracking performance for various force commands is validated.

II. System Overview

A. Compact Compliant Actuator with Piezoelectric Stacks

The CompAct^{TM}, shown in Fig. 1, is a series elastic actuator (SEA) made of a brushless motor coupled to a harmonic-drive gear and a custom-made elastic transmission system [7]. Unlike tradition SEA, the elastic element also incorporates a custom-made clutch forming a variable damping element forming a Variable Physical Damping Actuator (VPDA). The VPDA module integrated in the CompAct^{TM} provides on demand friction braking torque in parallel to the joint compliance. A PEA composed by four piezoelectric stacks provides the normal force to be delivered to the transmission clutch to generate the friction braking torque. By regulating the PEA force and therefore the friction torque on the basis of the velocity of the compliant element deflection damping regulation can be achieved. The force generated by piezoelectric stacks is sensed by means of a custom-made force sensor based on strain gauges which is placed at a base of the PEA system. To achieve precise physical damping regulation on the VPDA, it is very important that the force generated by the PEA system can be accurately and robustly controlled.

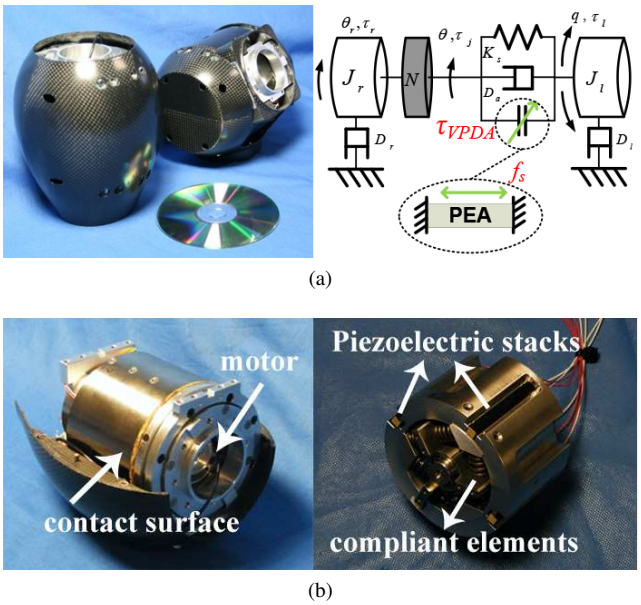

(a)

(b)

Fig. 1: The CompAct^{TM}: (a) overall system and its schematic diagram, where VPDA is actuated by the PEA; and (b) main elements inside the actuator.

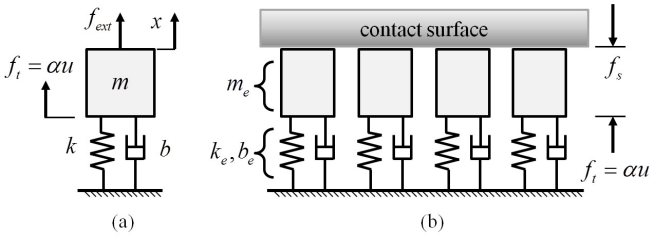

Fig. 2: Mechanical models: (a) a piezoelectric stack and (b) the PEA system with four piezoelectric stacks.

B. Dynamics of PEA System

The dynamic model of a single piezoelectric stack can be expressed as a combination of second order dynamics with nonlinear hysteresis [25]. Accordingly, the dynamics of the PEA system shown in Fig. 2 can be described as follows:

$$m_e\ddot{x} + b_e\dot{x} + k_e x + d = \alpha u + h(x,u) + f_s, \qquad (1)$$

where m_e, b_e, and k_e represent an effective mass, an effective damping and an effective stiffness of the PEA system, respectively, x, $\dot{x}$, and $\ddot{x}$ represent position, velocity and acceleration of the actuator, respectively, and d denotes an unknown external disturbances assumed to be bounded, while α denotes the electromechanical transformation ratio, u denotes the input voltage, $h(x,u)$ denotes nonlinearities from the hysteretic effect of piezoelectric stacks, and f_s denotes a sensed force measured between a contact surface and piezoelectric stacks.

III. Controller Design

A. Control Objectives

The target of the control is to allow the generated force from the PEA system to track a desired force trajectory. A force tracking error between the actual sensed force and the desired force is defined as

$$e_f \triangleq f_d - f_s, \qquad (2)$$

where f_d denotes the desired force trajectory.

An additive requirement in this paper is to minimise the computation demand for the force controller, because the control law will be physically implemented on a Digital Signal Processor (DSP) together with other motion control schemes for CompAct^{TM} system such as a motor position control, a damping estimator and a controller for the regulation of the VPDA system [7].

B. Controller Derivation

To control the PEA system by a voltage steering, the dynamic equation of the system shown in (1) is rearranged as

$$u = \alpha^{-1}(m_e\ddot{x} + b_e\dot{x} + k_e x + d - h(x,u)) + \alpha^{-1} f_s. \quad (3)$$

As a practical consideration, we introduce a positive constant value $\hat{\alpha}$ as an estimated value of α. Then, one can reformulate (3) as follows:

$$u = \eta(x, \dot{x}, \ddot{x}, u) + \hat{\alpha}^{-1} f_s, \quad (4)$$

where $\eta(x, \dot{x}, \ddot{x}, u)$ includes a force induced by all the nonlinearities of PEA system such as the hysteresis behaviour. This is defined by

$$\eta(x, \dot{x}, \ddot{x}, u) = \frac{1}{\alpha}[m_e\ddot{x} + b_e\dot{x} + k_e x + d - h(x,u)] + (\frac{1}{\alpha} - \frac{1}{\hat{\alpha}}) f_s, \quad (5)$$

where f_s can be regarded as a function of x when a dynamics of the contact surface such as a stiffness and a damping is considered. Hereinafter, for simplicity of the expression, η indicates $\eta(x, \dot{x}, \ddot{x}, u)$.

To achieve precise force tracking, the control voltage input is designed as

$$u = u_c + u_{servo}. \quad (6)$$

The first term of the right hand side of (6) involves cancelling out the nonlinearities of the system η such as the hysteresis and the creep effect in PEAs; and the second term is an auxiliary servo control to inject the desired error dynamics and to shape a transient response of the closed-loop system.

First, to select u_c, we use the TDE technique which indirectly performs an estimation of uncertain dynamics as follows:

$$u_c = \hat{\eta} \triangleq \eta_{(t-L)}, \quad (7)$$

where $\hat{\eta}$ denotes an estimation of η, L denotes an intentional time delay, and the subscript of $(t-L)$ denotes its value at the delayed time of L. Provided that L is sufficiently small, $\eta_{(t-L)}$ can be a good estimate of $\eta_{(t)}$ as follows:

$$\lim_{L \to 0} \eta_{(t-L)} \approx \eta_{(t)}. \quad (8)$$

This assumption holds because a sampled-data system can be treated as a continuous system when the sampling frequency is higher than 30 times than the system bandwidth [26]. Note that due to discontinuous nonlinearities, there exists an inevitable estimation error which is discussed in stability analysis.

From (4), the TDE for η can be obtained as follows:

$$\eta_{(t-L)} = u_{(t-L)} - \hat{\alpha}^{-1} f_{s(t-L)}. \quad (9)$$

A novelty of this controller is to use the TDE technique based on a force feedback, thus called force-based TDE. The corresponding stability is analyzed in Section IV.

Second, for the force-tracking of the system, the first-order desired force error dynamics is defined as

$$e_f + K_d \dot{e}_f = 0, \quad (10)$$

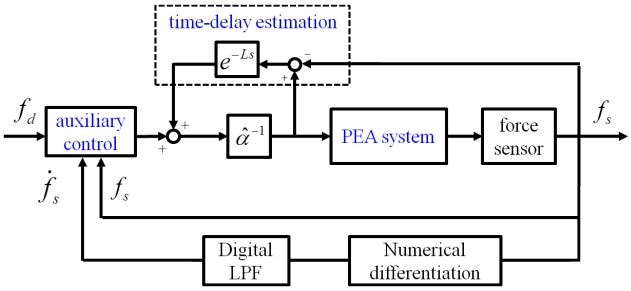

Fig. 3: Block diagram of the proposed force tracking controller.

where $\dot{e}_f \triangleq \dot{f}_d - \dot{f}_s$, and $\dot{f}_d$ and $\dot{f}_s$ denote the first derivatives of the desired force and the sensed force, respectively. This simple PD-type error dynamics is practically considered to minimise the computation demand for the control algorithm. Then, the auxiliary servo control in (6), u_{servo}, is selected to provide the above desired error dynamics to the force-controlled system as follows:

$$u_{servo} \triangleq \hat{\alpha}^{-1}(f_d + K_d \dot{e}_f). \quad (11)$$

Finally, by combining (6), (7), (9), and (11), the force tracking control using force-based TDE is summarized as

$$u = \underbrace{u_{(t-L)} - \hat{\alpha}^{-1} f_{s(t-L)}}_{\text{force-based TDE}} + \underbrace{\hat{\alpha}^{-1}(f_d + K_d \dot{e}_f)}_{\text{PD-type servo control}}. \quad (12)$$

C. Discussion on the Proposed Controller

As seen in the above equation, the terms of proposed controller has clear meaning. The force-based TDE is used to compensate for the nonlinearities of the PEA system including hysteresis and unmodeled dynamics without a mathematical model; hence this makes the proposed control simple and model-free. The PD-type force feedback leads the PEA system to accurately follow the desired force trajectory by adjusting the gain K_d. Thanks to the simple structure of the control law, its required computation effort is no more than that of conventional PID control, making it computationally efficient.

For a physical implementation, a first-order digital low-pass filter is practically utilized to reduce a noise of the fisrt derivative of f_s as a minimum use of the filter. In the controller, the selection of $\hat{\alpha}^{-1}$ significantly affects the control performance. Theoretically, the best selection of $\hat{\alpha}^{-1}$ is a nominal value of α, the electromechanical transformation ratio between the control voltage and the generated force of PEA. However, for more practicality, $\hat{\alpha}^{-1}$ is tuned by increasing from a small positive value until the system shows an oscillating response. Detailed discussion on the controller gains $\hat{\alpha}^{-1}$ and K_d can be found in the following section, i.e., stability analysis. Additionally, for more clear description of the proposed controller, a block diagram is illustrated in Fig. 3.

IV. Stability Analysis

By substituting (6) and (7) into the system dynamics (4), a closed-loop dynamics of the system is obtained as

$$e_f + K_d \dot{e}_f = \epsilon \quad (13)$$

with

$$\epsilon \triangleq \hat{\alpha}(\eta - \hat{\eta}), \tag{14}$$

which denotes a residual error after applying the force-based TDE. Accordingly, it is natural to show a boundedness of this residual error ϵ for a stability proof of the closed-loop system.

From (6), (7), and (4), the residual error (14) can be expressed as

$$\epsilon = \hat{\alpha} u_{servo} - f_s. \tag{15}$$

A combination of (1) and (15) yields

$$\epsilon = \hat{\alpha} u_{servo} + \xi - \alpha u \tag{16}$$

with

$$\xi \triangleq m_e \ddot{x} + b_e \dot{x} + k_e x + d - h(x, u). \tag{17}$$

Substituting (6) and (7) into (16) gives

$$\epsilon = (\hat{\alpha} - \alpha) u_{servo} + \xi - \alpha \hat{\eta}_{(t-L)}. \tag{18}$$

Then, from (5) and (17), equation (18) can be represented as follows:

$$\begin{aligned} \epsilon &= (\hat{\alpha} - \alpha) u_{servo} - (1 - \alpha/\hat{\alpha}) f_{s(t-L)} + \xi - \xi_{(t-L)} \\ &= (\hat{\alpha} - \alpha) u_{servo} - (1 - \alpha/\hat{\alpha}) f_{s(t-L)} + \phi, \end{aligned} \tag{19}$$

where $\phi \triangleq \xi - \xi_{(t-L)}$, which can be derived from (17) as

$$\begin{aligned} \phi = m_e[\ddot{x} - \ddot{x}_{(t-L)}] + b_e[\dot{x} - \dot{x}_{(t-L)}] + k_e[x - x_{(t-L)}] \\ + [d - d_{(t-L)}] + [h(x, u) - h(x, u)_{(t-L)}]. \end{aligned} \tag{20}$$

In (20), it is important to notice that the hysteresis operator $h(x, u)$ is not a smooth function, but a Lipschitz-continuous function [27]. The uncertain external disturbance d is discontinuous but bounded, and $\ddot{x}$ can be assumed to be bounded because we consider the PEA system is physically constrained to the contact surface as shown in Fig. 2. Therefore, the term ϕ can be divided into smooth (continuous and differentiable), Lipschitz-continuous, and bounded terms as follows:

$$\phi = \phi_s + \phi_l + \phi_b, \tag{21}$$

where

$$\phi_s = b_e[\dot{x} - \dot{x}_{(t-L)}] + k_e[x - x_{(t-L)}], \tag{22}$$

$$\phi_l = -h(x, u) + h(x, u)_{(t-L)}, \tag{23}$$

$$\phi_b = m_e[\ddot{x} - \ddot{x}_{(t-L)}] + [d - d_{(t-L)}]. \tag{24}$$

If the boundedness and smoothness condition of $(b_e \dot{x} + k_e x)$ are satisfied, $\phi_s = O(L^2)$ as shown in [28]. From the Lipshitz-continuous condition, we can obtain that $\phi_l = O(L)$. In addition, it is clear that $|\phi_b| \leq \delta$, where δ is a positive constant value. Therefore, ϕ is bounded by $|\phi| \leq \delta + O(L)$ for a sufficient small L.

Substituting $f_{s(t-L)} = u_{servo(t-L)} - \epsilon_{(t-L)}$ from (15) into (19) yields

$$\epsilon = (1 - \alpha/\hat{\alpha}) \epsilon_{(t-L)} + \psi + \phi, \tag{25}$$

where $\psi = (\alpha - \hat{\alpha})(u_{servo} - u_{servo(t-L)})$. Then, the above equation can be expressed in the discrete-time domain as follows:

$$\epsilon_{(k)} = (1 - \alpha/\hat{\alpha}) \epsilon_{(k-1)} + \psi_{(k)} + \phi_{(k)}, \tag{26}$$

where the subscript k denotes its value of the k^{th} sampling time. With respect to $\epsilon_{(k)}$, $\psi_{(k)}$ and $\phi_{(k)}$ are forcing functions which are bounded for a sufficient small sampling period L. Therefore, if the root of $(1 - \alpha/\hat{\alpha})$ resides inside a unit circle, the equation (26) is ultimately bounded as

$$|\epsilon| \leq \sigma, \tag{27}$$

where σ is a positive value. The residual error after the force-based TDE can become small by reducing the sampling period L, as deduced from (8).

Finally, the closed-loop error dynamics is rearranged from (13) as

$$\dot{e}_f + {K_d}^{-1} e_f = {K_d}^{-1} \epsilon. \tag{28}$$

Because ${K_d}^{-1} \epsilon$ is bounded to a small value, the overall system is bounded-input-bounded-output (BIBO) stable, i.e., $\lim_{t \to \infty} |e_{f(t)}| \leq K_d^{-1} \sigma$.

As shown in (28), the gain K_d determines a convergence speed of the closed-loop system response. Thus, the gain is set as a desired time constant. One can find that even though very small K_d gain, the stability of the controller is still guaranteed and the force response converges to the desired trajectory quickly. However, if K_d becomes smaller, the effect of the residual error ϵ is increased. Conversely, large K_d can reduce the effect of ϵ but it may amplify a noise effect of the derivative of the sensed force, $\dot{f}_s$. Note that $\dot{f}_s$ is easily contaminated by the noise of the sensed force and the numerical differentiation in a real situation. Indeed, K_d is experimentally selected by a user to achieve a compromise among convergence speed, tracking accuracy, and noisy response.

V. EXPERIMENTAL VERIFICATION

A. Experiment Setting

The proposed force tracking controller is physically implemented on the PEA of CompAct™ system. The PEA system consists of four piezoelectric stacks, Noliac SCMAP04, with a size of 56×5×5 mm, weight of 12 g and stroke of 82.2 μm. A custom-made force sensor based on a strain gauge is mounted for the sensing of the force applied by the PEA system. The noise of the sensed force was measured as the root-mean-squared value (RMS) of 0.307 N.

The control hardware is provided with a motor control board equipped with a Motorola DSP 56F8000 chip running at a sampling frequency of 1 kHz. Data acquisition is executed using 12-bit analog-to-digital converters while the analogue control input to the piezoelectric driver amplifier is generated by 12-bit digital-to-analog converters. The latter board is used for amplifying the control signals for the PEA system in the nominal voltage range of [0, 160] V.

The settings of the proposed force controller are as follows: the controller gains in (12) are selected as $\hat{\alpha}^{-1} = 0.15$

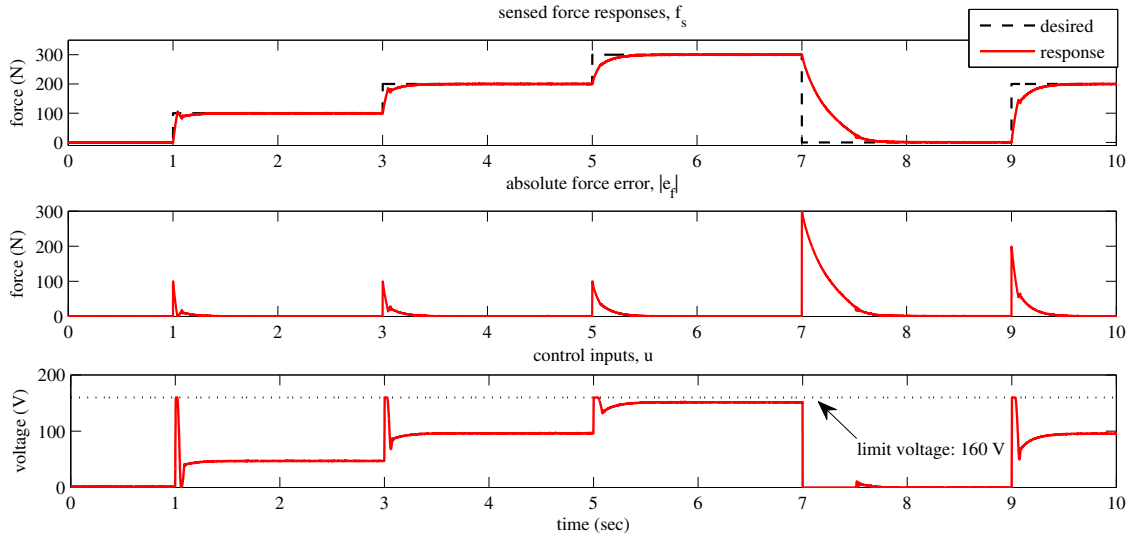

Fig. 4: Step responses of the proposed force controller.

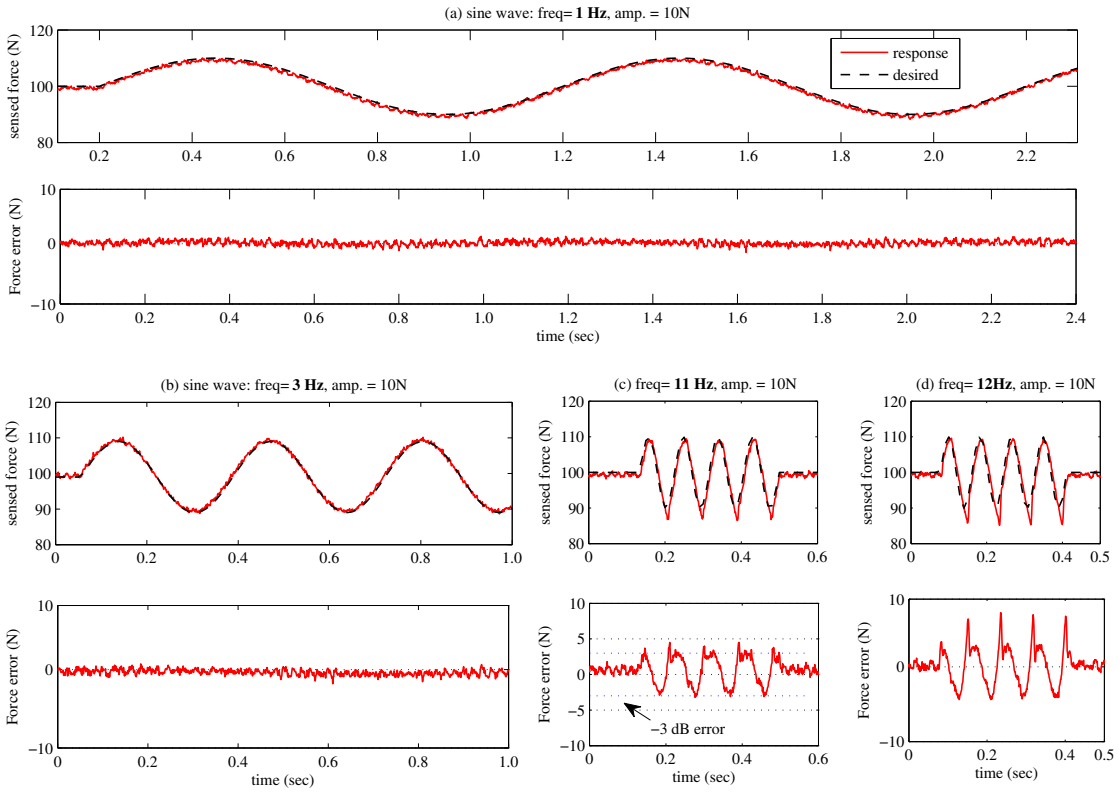

Fig. 5: Sinusoidal reference responses of the proposed force controller.

and $K_d = 0.1$. The sampling period of the DSP is set to 1 ms; thus, $L = 1$ ms. The time-delayed values of the force-based TDE, $u_{(t-L)}$ and $f_{s(t-L)}$, can be efficiently obtained by using the stored values of u and f_s in the previous sampling. The derivative of e_f is calculated by the numerical differentiation with the backward difference as $\dot{e}_{f(t)} = (e_{f(t)} - e_{f(t-L)})L^{-1}$.

B. Results

The performance of the proposed force control is investigated for different reference inputs. Figure 4 shows the regulation performance of the proposed control with respect to various step commands. Throughout the experiment, RMS values of the steady-state error are observed as no more than 0.39 N. In the transient response, no severe overshoot

TABLE I: Results on Sinusoidal Commands

freq.	max. error	RMS error
1 Hz	1.8 N	0.729 N
3 Hz	2.1 N	0.818 N
11 Hz	4.5 N	2.248 N
12 Hz	8.1 N	3.069 N

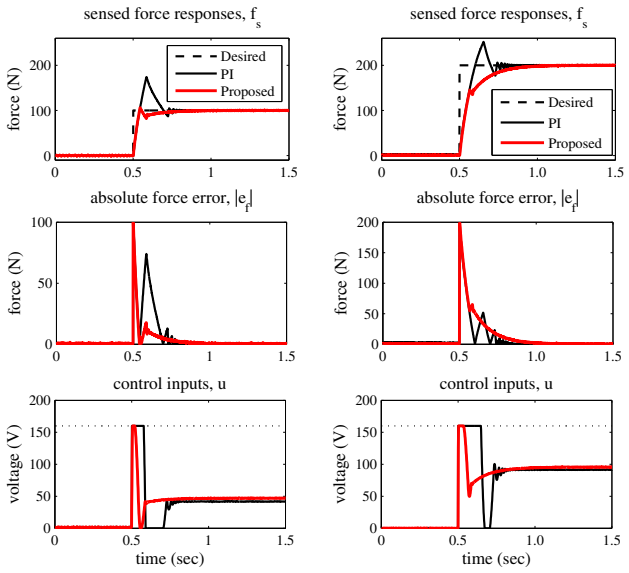

Fig. 6: Experimental results on comparing with PI controller: (a) 100 N step command and (b) 200 N step command, where the blue-solid line denotes the step response of the PI controller, the red-solid line denotes that of the proposed controller and the black-dotted line denotes the desired value.

is observed, which is one of undesirable response normally resulted from the creep effect of PEAs [29]. The peaks and sudden changes of the control input just after t=1, 3, 5, 7.5, and $9s$ imply that the proposed control operates to quickly compensate the delayed behavior of PEA resulted from the phase transformation in the piezoelectric material. Hence, it is confirmed that the hysteresis and creep behavior of the PEA system is effectively compensated by the force-based TDE in the proposed controller. Furthermore, the control input has no serious oscillation in spite of the use of the force derivative in (12). This verifies that the proposed controller is practically implementable to the real system.

The validation of the tracking performance of the proposed control, is investigated by sending to the experimental setup sinusoidal references with different frequencies from 1 to 12 Hz with the amplitude of 10 N, $f_d(t) = 100 + 10\sin(2\pi f_q t)$, where f_q denotes the frequency of the trajectory. As shown in Fig. 5, the PEA system shows a better performance in the low frequency. The results are summarized in Table. I. The approximated bandwidth of the controller is confirmed as 11 Hz under the stroke of 20 N and the preload of 100 N .

C. Comparison Study with PI controller

To validate the effectiveness of the proposed controller, we demonstrate experimental comparisons to a PI-force controller represented by

$$u = K_p e_f + K_i \int e_f dt. \tag{29}$$

For a fair comparison, gains of the PI controller are tuned as $K_p = 2.67 \times 10^{-3}$ and $K_i = 0.11 \times 10^{-3}$, which are managed to be tuned to have the fastest convergence and smallest steady-state error, by trial and error.

Interestingly, figures 6 (a) and (b) show that the results of best-tuned PI control also quickly converge to each desired force with small steady-state error: for instance, its RMS value for 100 N step command after t=1s is 0.426 N, while that of the proposed control is 0.384 N. However, large overshoots are observed as 74.1 % for 100 N step command and 51.7 % for 200 N step command, while those of the proposed control are 6.1 % and 0.1 %, respectively. This overshoot of PI control was very difficult to be removed. A consistent result when applying PI controller to the PEA can be found in [29], which is mostly caused by creep effect of the PEA. Therefore, it is confirmed by the above experimental results that the proposed control can effectively compensate the hysteresis and creep effect thanks to force-based TDE and provide fast but smooth force tracking performance.

VI. CONCLUSIONS

This work has proposed a method of implementing precise force tracking performance for a piezoelectric actuator system incorporated into the recent development of CompAct^{TM}. The force-based time-delay estimation is proposed to compensate nonlinearities arising the hysteresis of piezoelectric stacks, with small computation efforts. The simple proportional-derivative type force feedback enables the quick and smooth transient response. The experiment results on PEA system mounted on the CompAct^{TM} show that the proposed controller performs precise and robust force tracking without using mathematical model. Our future work will focus on an application study of realizing desired physical damping behavior to CompAct^{TM} arm system by using the proposed controller. A preliminary result is introduced in a companion paper submitted to ICRA 2014 [30]. In addition, a possible extension of the current scheme is to find a way to reduce the effect of the residual error ϵ for more accurate tracking performance.

ACKNOWLEDGMENT

This work is supported by the European Community, within the FP7 ICT-287513 SAPHARI project and partly supported by Basic Science Research Program through the National Research Foundation of Korea(NRF) funded by the Ministry of Education (2013R1A6A3A03062246).

REFERENCES

[1] B.-S. Kim and J.-B. Song, "Hybrid dual actuator unit: A design of a variable stiffness actuator based on an adjustable moment arm mechanism," in *Proceedings of 2010 IEEE International Conference on Robotics and Automation (ICRA)*. IEEE, 2010, pp. 1655–1660.

[2] J. Oblak and Z. Matjačić, "Design of a series visco-elastic actuator for multi-purpose rehabilitation haptic device," *Journal of neuroengineering and rehabilitation*, vol. 8, no. 1, p. 3, 2011.

[3] A. M. Dollar and R. D. Howe, "A robust compliant grasper via shape deposition manufacturing," *IEEE/ASME Transactions on Mechatronics*, vol. 11, no. 2, pp. 154–161, 2006.

[4] N. Lauzier and C. Gosselin, "Series clutch actuators for safe physical human-robot interaction," in *Proceedings of 2011 IEEE International Conference on Robotics and Automation (ICRA)*. IEEE, 2011, pp. 5401–5406.

[5] L. C. Visser, R. Carloni, and S. Stramigioli, "Energy-efficient variable stiffness actuators," *IEEE Transactions on Robotics*, vol. 27, no. 5, pp. 865–875, 2011.

[6] M. Laffranchi, N. G. Tsagarakis, and D. G. Caldwell, "A variable physical damping actuator (vpda) for compliant robotic joints," in *the 2010 IEEE International Conference on Robotics and Automation (ICRA)*. IEEE, 2010, pp. 1668–1674.

[7] M. Laffranchi, N. Tsagarakis, and D. G. Caldwell, "A compact compliant actuator (CompAct^{TM}) with variable physical damping," in *Proceedings of 2011 IEEE International Conference on Robotics and Automation (ICRA)*. IEEE, 2011, pp. 4644–4650.

[8] M. Laffranchi, N. G. Tsagarakis, and D. G. Caldwell, "Analysis and development of a semiactive damper for compliant actuation systems," *Mechatronics, IEEE/ASME Transactions on*, vol. 18, no. 2, pp. 744–753, 2013.

[9] B. Ugurlu, N. G. Tsagarakis, E. Spyrakos-Papastavridis, and D. G. Caldwell, "Compliant joint modification and real-time dynamic walking implementation on bipedal robot ccub," in *Proceedings of 2011 IEEE International Conference on Mechatronics (ICM)*. IEEE, 2011, pp. 833–838.

[10] A. Radulescu, M. Howard, D. J. Braun, and S. Vijayakumar, "Exploiting variable physical damping in rapid movement tasks," in *Proceedings of 2012 IEEE/ASME International Conference on Advanced Intelligent Mechatronics (AIM)*. IEEE, 2012, pp. 141–148.

[11] J. Peng and X. Chen, "A survey of modeling and control of piezoelectric actuators," *Modern Mechanical Engineering*, vol. 3, no. 1, pp. 1–20, 2013.

[12] M. Goldfarb and N. Celanovic, "Modeling piezoelectric stack actuators for control of micromanipulation," *Control Systems, IEEE*, vol. 17, no. 3, pp. 69–79, 1997.

[13] G. Song, J. Zhao, X. Zhou, and J. A. De Abreu-García, "Tracking control of a piezoceramic actuator with hysteresis compensation using inverse preisach model," *IEEE/ASME Transactions on Mechatronics*, vol. 10, no. 2, pp. 198–209, 2005.

[14] Y. Chen, J. Qiu, J. Palacios, and E. C. Smith, "Tracking control of piezoelectric stack actuator using modified Prandtl-Ishlinskii model," *Journal of Intelligent Material Systems and Structures*, vol. 24, no. 6, pp. 753–760, 2013.

[15] M. Ismail, F. Ikhouane, and J. Rodellar, "The hysteresis Bouc-Wen model, a survey," *Archives of Computational Methods in Engineering*, vol. 16, no. 2, pp. 161–188, 2009.

[16] F. Szufnarowski and A. Schneider, "Force control of a piezoelectric actuator based on a statistical system model and dynamic compensation," *Mechanism and Machine Theory*, vol. 46, no. 10, pp. 1507–1521, 2011.

[17] S.-B. Choi and C.-H. Lee, "Force tracking control of a flexible gripper driven by piezoceramic actuators," *Journal of dynamic systems, measurement, and control*, vol. 119, no. 3, pp. 439–446, 1997.

[18] M. Rakotondrabe, C. Clévy, and P. Lutz, "Modelling and robust position/force control of a piezoelectric microgripper," in *Proceedings of 2007 IEEE International Conference on Automation Science and Engineering (CASE)*. IEEE, 2007, pp. 39–44.

[19] S. Yu, G. Alici, B. Shirinzadeh, and J. Smith, "Sliding mode control of a piezoelectric actuator with neural network compensating rate-dependent hysteresis," in *Proceedings of the 2005 IEEE International Conference on Robotics and Automation (ICRA)*. IEEE, 2005, pp. 3641–3645.

[20] W. Li and X. Chen, "Compensation of hysteresis in piezoelectric actuators without dynamics modeling," *Sensors and Actuators A: Physical*, 2013.

[21] K. Abidi, A. Sabanovic, and S. Yesilyurt, "Sliding-mode based force control of a piezoelectric actuator," in *Proceedings of the 2004 IEEE International Conference on Mechatronics (ICM)*. IEEE, 2004, pp. 104–108.

[22] K. Youcef-Toumi and F. Kondo, "Time delay control," in *American Control Conference, 1989*. IEEE, 1989, pp. 1912–1917.

[23] M. Jin, Y. Jin, P. H. Chang, and C. Choi, "High-accuracy tracking control of robot manipulators using time delay estimation and terminal sliding mode," *International Journal of Advance Robotic Systems*, vol. 8, no. 4, pp. 65–78, 2011.

[24] J. Lee, C. Yoo, Y.-S. Park, B. Park, S.-J. Lee, D.-G. Gweon, and P.-H. Chang, "An experimental study on time delay control of actuation system of tilt rotor unmanned aerial vehicle," *Mechatronics*, vol. 22, no. 2, pp. 184–194, 2012.

[25] H. Adriaens, W. L. De Koning, and R. Banning, "Modeling piezoelectric actuators," *IEEE/ASME Transactions on Mechatronics*, vol. 5, no. 4, pp. 331–341, 2000.

[26] G. F. Franklin, M. L. Workman, and D. Powell, *Digital control of dynamic systems*. Addison-Wesley Longman Publishing Co., Inc., 1997.

[27] H. Logemann, E. P. Ryan, and I. Shvartsman, "A class of differential-delay systems with hysteresis: asymptotic behaviour of solutions," *Nonlinear Analysis: Theory, Methods & Applications*, vol. 69, no. 1, pp. 363–391, 2008.

[28] W. Su, S. Drakunov, and U. Ozguner, "An O(T2) boundary layer in sliding mode for sampled-data systems," *IEEE Transactions on Automatic Control*, vol. 45, no. 3, pp. 482–485, 2000.

[29] H. Jung, J. Y. Shim, and D. Gweon, "Tracking control of piezoelectric actuators," *Nanotechnology*, vol. 12, no. 1, p. 14, 2001.

[30] N. Kashiri, M. Laffranchi, J. Lee, N. G. Tsagarakis, L. Chen, and D. G. Caldwell, "Real-time damping estimation for variable impedance actuator," in *Proceedings of the 2014 IEEE International Conference on Robotics and Automation (ICRA)*. IEEE, 2014, (Accepted).